Stress Analysis of Steam-Methane Reformer Tubes

by

Muhammad Hazri Bin Idris

Dissertation submitted in partial fulfilment of
the requirement for the
Bachelor of Engineering (Hons)
(Mechanical Engineering)

MAY 2011

Universiti Teknologi PETRONAS
Bandar Seri Iskandar
31750 Tronoh
Perak Darul Ridzuan

CERTIFICATION OF APPROVAL

Stress Analysis of Steam Methane Reformer Tubes

by

Muhammad Hazri Bin Idris

A project dissertation submitted to the
Mechanical Engineering Programme
Universiti Teknologi PETRONAS
in partial fulfilment of the requirement for the
BACHELOR OF ENGINEERING (Hons)
(MECHANICAL ENGINEERING)

Approved by,

(Dr. Azmi Abdul Wahab)

UNIVERSITI TEKNOLOGI PETRONAS
TRONOH, PERAK
MAY 2011

CERTIFICATION OF ORIGINALITY

This is to certify that I am responsible for the work submitted in this project, that the original work is my own except as specified in the references and acknowledgements, and that the original work contained herein have not been undertaken or done by unspecified sources or persons.

MUHAMMAD HAZRI BIN IDRIS

ABSTRACT

Steam-methane reformer tubes operate at temperature exceeding 800°C and are designed to last about 100,000 hours of service. However, the life achieved can be significantly shorter due to creep failure of the reformer tube. In order to reliably predict the performance of the tube, good estimation of the stresses acting at any point along the tube length and thickness is required. Finite Element Method (FEM) will be used to perform the stress analysis of the tube and the analysis will consider the variation in stresses along the tube length and thickness due to temperature and pressure differences, in addition to service life. The analysis was conducted by using ANYSY software. The model is a two dimensional axisymmetric model. The main advantage to use a 2D axisymmetric model compared to a full 3D model is the reduced calculation time and it is easier to change subtle details to the geometry. Two different types of analyses were conducted; stress analysis due to internal pressure and stress analysis due to difference in temperature along the tube. For the first analysis, it was shown that the Von Misses Stress is highest at the inner wall of the tube and lowest at the outer wall. For the second analysis, it was shown that the Von Misses Stress is highest at the inner wall of the tube and lowest at the middle of the tube. The Von Misses Stress is decreasing from inner wall to the middle wall but then increasing to the outer wall.

ACKNOWLEDGMENT

First of all, the author would like to express utmost gratitude and appreciation to Allah because with His blessings and help, the Final Year Project went very smoothly. Alhamdulillah, all praises to Him that the author have been able to complete this project on time.

This project would not have been possible without the assistance and guidance of certain individuals and organization whose contributions have helped in its completion. First and foremost, the author would like to express his sincere thanks and utmost appreciation to the project supervisor, Dr. Azmi Abdul Wahab for having faith and strong support in guiding the author throughout the whole period of completing the final year project. His kind assistance and guidance from the beginning to the end of this study really help me to undergo my project successfully.

Special express gratitude is also reserved for the Mechanical Engineering Department of Universiti Teknologi PETRONAS for providing excellent support in terms of providing cutting edge knowledge and information not just within the Final Year Project but also the five years spent undergoing every single bit of invaluable knowledge on mechanical engineering.

The author would also like to deliver his warmth appreciation to other lecturer, namely Dr. Mokhtar Awang for assisting with the technical support and guidance towards this project.

Finally many thanks to the author's family and fellow colleagues for their help and ideas throughout the completion of this study. I hope that the outcome of this report will bring beneficial output to others as well. Thank you very much everyone.

CHAPTER 1

INTRODUCTION

1.1 Background of study

Hydrogen, H_2 is the most abundant element on the planet. There are various functions of hydrogen gas such as fuel for the mobile and stationary power generation by using fuel cell. One of the advantage of hydrogen gas is it is an environmental friendly fuel that does not emit carbon dioxide which is known as one of the global warming gases. Since that, research activities on hydrogen gas production increase rapidly as the demand of this gas is expected to be increased in the near future.

A steam reformer is a device based on steam reforming or autothermal reforming and is used in chemical engineering, which can produce pure hydrogen gas from natural gas using a catalyst. Natural gas contains methane (CH_4) that can be used to produce hydrogen via thermal processes. There are two natural gas reformer technologies which are autothermal reforming (ATR) and steam methane reforming (SMR). Both methods work by exposing natural gas to a catalyst which is usually nickel at high temperature and pressure. (www.assemblymag.com, 2004)

Steam methanereforming (SMR) is the most common method of producing commercial bulk hydrogen as well as the hydrogen used in the industrial synthesis of ammonia. It is also the least expensive method.(George W. Crabtree, Mildred S. Dresselhaus, and Michelle V. Buchanan, 2004)

1.2 Problem Statement

In methanol processing plants, steam-methane reformers consist of hundreds of vertical tubes operating at temperatures up to 1000°C. When metals are subjected to stress at a high temperature, a type of plastic deformation known as creep occurs. This deformation takes place over an extended period of time and failure is due to either excessive deformation of the components or physical separation of the affected parts. The component which typically fails by creep is the steam-methane reformer tube. The tube material is commonly centrifugally cast austenitic stainless steel, and these tubes typically fail via creep void formation and coalescence during service.

According to Baher El Shaikh(2010)

> The creep damage occurs over the complete circumference (or at least a large part of the circumference) and over a longer (axial) part of the tube. The damage process results in diameter increase and creep damage (cavitation) at the inner diameter. (p.6)

The life expectancy of these tubes is 100,000 hours or 11.4 years. However the actual lives achieved can be significantly shorter than the target. (Ashok Kumar Ray et al,2003). Thus, there are two major concerns which are the cost of replacing these tubes which the price of a tube is about US$7000 and the associated cost of a plant shutdown.

1.3 Objective and Scope of Study

The objective of this project is to perform stress analysis of steam methane reformer (SMR) tubes by using finite element method. By doing this, the author can estimate the stresses acting at any point along the tube length and thickness and the results can be used to minimize potential future failures and economic losses because of the reformer shutdowns.

The scope of study of this project is started by the tube model has been divided into The tube has been divided into 5 sections and analyzed all the 5 points along the tubes. Each sections has 2.5 m of length interval. Two types of analysis has been conducted which are stress analysis and thermal stress analysis.Stress analysis has been conducted by applying internal pressure to the tube while thermal stress analysis has been conducted by applying temperature distribution and internal pressure along the tube.The result has been validated by comparing the Von Misses Stress of the FEM with the analytical result.

CHAPTER 2

LITERATURE REVIEW

2.1 Steam-Methane Reforming (SMR) Process

The steam methane reforming (SMR) process consists of two steps.

1. Reforming of natural gas

   The first step of the SMR process involves methane reacting with steam at 750-800°C to produce a synthesis gas (syngas), a mixture primarily made up of hydrogen (H_2) and carbon monoxide (CO).

   $$CH_4 + H_2O \rightarrow CO + 3\ H_2$$

2. Shift Reaction

   The second step is known as a water gas shift (WGS) reaction. In this step, the carbon monoxide produced in the first reaction is reacted with steam over a catalyst to form hydrogen and carbon dioxide (CO_2). This process occurs in two stages, consisting of a high temperature shift (HTS) at 350°C and a low temperature shift (LTS) at 190-210°C.

   $$CO + H_2O \rightarrow CO_2 + H_2$$

There are small quantities of carbon monoxide, carbon dioxide, and hydrogen sulphide in hydrogen produced from the reforming process as impurities and depending on use, may require further purification. The primary steps for purification include:

- Feedstock purification

  This process removes poisons, including sulfur (S) and chloride (Cl), to increase the life of the downstream steam reforming and other catalyst.

- Product purification

  In a liquid absorption system, CO_2 is removed. The product gas undergoes a methanation step to remove residual traces of carbon oxides.

2.2 Steam Methane Reformer Tube

The tube is made of Schmidt-Clemens Centralloy CA4852-Micro material. The data for CA4852-Micro were taken from Schmidt-Clemens Materials Datasheet (Schmidt-Clemens, 2001). The physical properties and mechanical properties of the material are as follows:

Density, $\rho = 8.0$ g/cm^3

Thermal Conductivity, k =14.6 W/mK

Poisson's ratio, v =0.3

Young's Modulus of Elasticity: Varies with the temperature

2.3 Creep Failure

According to John Brightling (2002),

> The main damage mechanism for reformer tubes is the combination of thermal stresses through the tube wall and the stress imposed by operation under pressure. This combination causes creep damage, which typically develops on or just below the inside surface.

David N. French (1991) says that creep may be defined as a time-dependent deformation at elevated temperature and constant stress and a failure from such a condition is referred to as a creep failure or, occasionally, a stress rupture. The temperature at which creep begins depends on the alloy composition.

The end of useful service life of the high-temperature components in a boiler is usually a failure by a creep or stress-rupture mechanism. The root cause may not be elevated temperature, as fuel-ash corrosion or erosion may reduce the wall thickness so that the onset of creep and creep failures occur sooner than expected.In a superheater or reheater tube, often the very first sign of creep damage is longitudinal cracks in the steam-side scale.

Figure 2.1: Crack/Creep failure on a gas pipe

2.4 Finite Element Analysis (FEA)

The FEA method has wide application and enjoys extensive utilization in the structural, thermal and fluid analysis areas.

According to Steve Roensch(2008), this method is comprised of three major phases:

1. Pre-processing

   The analyst develops a finite element mesh to divide the subject geometry into sub domains for mathematical analysis, and applies material properties and boundary conditions
2. Solution

   The program derives the governing matrix equations from the model and solves for the primary quantities
3. Post-processing

   The analyst checks the validity of the solution, examines the values of primary quantities (such as displacements and stresses), and derives and examines additional quantities (such as specialized stresses and error indicators).

2.5 Analytical Equation

There are also some analytical equations that to be calculated in this project which are thermal stresses, stresses due to internal pressure, stresses due to tube weight and lastly Von Misses Stress.

2.5.1 Thermal Stresses Calculation

Consider a long thick-walled cylinder symmetric about the tube axis as shown in Figure 2.2 with a tube wall temperature distribution of $T=T(r)$.

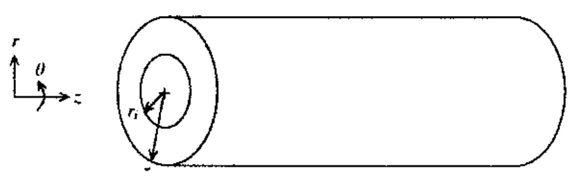

Figure 2.2: Long Thick-Walled Cylinder

The hoop, radial and axial thermal stresses are given by the following equations (Morozov, 1964):

$$\sigma_\theta = \frac{\alpha E}{1-\nu}\left[\left(1+\frac{r_i^2}{r^2}\right)\left(\frac{1}{r_o^2-r_i^2}\right)\int_{r_i}^{r_o} Tr\,dr + \frac{1}{r^2}\int_{r_i}^{r} Tr\,dr - T\right]$$

$$\sigma_r = \frac{\alpha E}{1-\nu}\left[\left(1-\frac{r_i^2}{r^2}\right)\left(\frac{1}{r_o^2-r_i^2}\right)\int_{r_i}^{r_o} Tr\,dr - \frac{1}{r^2}\int_{r_i}^{r} Tr\,dr\right]$$

$$\sigma_z = \frac{\alpha E}{1-\nu}\left[\left(\frac{2}{r_o^2-r_i^2}\right)\int_{r_i}^{r_o} Tr\,dr - T\right]$$

where: α =coefficient of thermal expansion

E = modulus of elasticity

$T=T(r)$= temperature distribution

ν = Poisson's ratio=0.3 (assumed constant)

r_i= internal radius

r_o= external radius

Assuming a steady heat flux through the wall, with α, E and ν also being constant across the wall, the hoop, radial and axial thermal stresses can be approximated by (Morozov,1964):

$$\text{hoop stress: } \sigma_{hT} = \frac{\alpha E(T_i - T_o)}{2(1-\nu)}\left[\frac{1-\ln\left(\frac{r_o}{r}\right)}{\ln\left(\frac{r_o}{r_i}\right)} - \frac{\left(\frac{r_o}{r}\right)^2+1}{\left(\frac{r_o}{r_i}\right)^2-1}\right]$$

$$\text{radial stress: } \sigma_{rT} = \frac{\alpha E(T_i - T_o)}{2(1-\nu)}\left[\frac{-\ln\left(\frac{r_o}{r}\right)}{\ln\left(\frac{r_o}{r_i}\right)} + \frac{\left(\frac{r_o}{r}\right)^2-1}{\left(\frac{r_o}{r_i}\right)^2-1}\right]$$

$$\text{axial stress: } \sigma_{aT} = \frac{\alpha E(T_i - T_o)}{2(1-\nu)}\left[\frac{1-2\ln\left(\frac{r_o}{r}\right)}{\ln\left(\frac{r_o}{r_i}\right)} - \frac{2}{\left(\frac{r_o}{r_i}\right)^2-1}\right]$$

where: T_i=internal temperature

T_0=external temperature

r = radial distance to point of interest.

(Other variables as defined earlier)

2.5.2Stresses due to Internal Pressure

There is no outer pressure used in this analysis. Thus, according to Lame's equation, the hoop, radial and axial stresses due to internal pressure, p in a long thick-walled cylinder {Muvdi, 1991}

$$\text{hoop stress: } \sigma_{hp} = \frac{pr_i^2}{r_o^2 - r_i^2}\left(1+\frac{r_o^2}{r^2}\right)$$

$$\text{radial stress: } \sigma_{rp} = \frac{pr_i^2}{r_o^2 - r_i^2}\left(1-\frac{r_o^2}{r^2}\right)$$

$$\text{axial stress: } \sigma_{ap} = \frac{pr_i^2}{r_o^2 - r_i^2}$$

where: p = internal pressure.

(Other variables as defined earlier)

2.5.3 Stresses due to Tube Weight

Tube hangar system supports seventy five percent of tube weight. The axial stress due to tube weight is:

$$\text{axial stress}: \quad \sigma_{aW} = 0.25\times\frac{W}{A} = 0.25\times\frac{\rho g A l}{A} = 0.25\times\rho g l$$

$$\begin{array}{c}\text{axial stress per}\\ \text{length of tube}\end{array}: \quad \frac{\sigma_{aW}}{l} = -19.62\times10^{-3}\,\text{MPa/m}$$

where: W=weight of tube

A=cross sectional area of tube

P=density of reformer tube=8000kg/m^3 (Schmidt+ Clemens, 2001)

g = gravitational acceleration= 9.81 m/s^2

l = vertical distance from top flange to point of interest.

Negative sign indicates compressive stress.

2.5.4 Calculation of Effective Stress

Effective stress (to be referred in this report as Von Misses Stress) was calculated using the Von Misses Stress criterion as follow (www.engineersedge.com,2010)

$$\sigma_v = \sqrt{\frac{(\sigma_1-\sigma_2)^2+(\sigma_2-\sigma_3)^2+(\sigma_1-\sigma_3)^2}{2}}$$

where:

$$\sigma_1 = \sigma_{hT} + \sigma_{hP}$$
$$\sigma_2 = \sigma_{rT} + \sigma_{rP}$$
$$\sigma_3 = \sigma_{aT} + \sigma_{aP} + \sigma_{aW}$$

(Principal stresses from combined hoop, radial and axial stresses)

CHAPTER 3

METHODOLOGY

3.1 Tools and Equipment

The followings are the major tools will be used in the analysis of this project:

- ANSYS simulation software
- MATLAB software
- Microsoft Excel

3.2 Project Flowchart

The overall flow of the project is depicted in Figure 3.1.

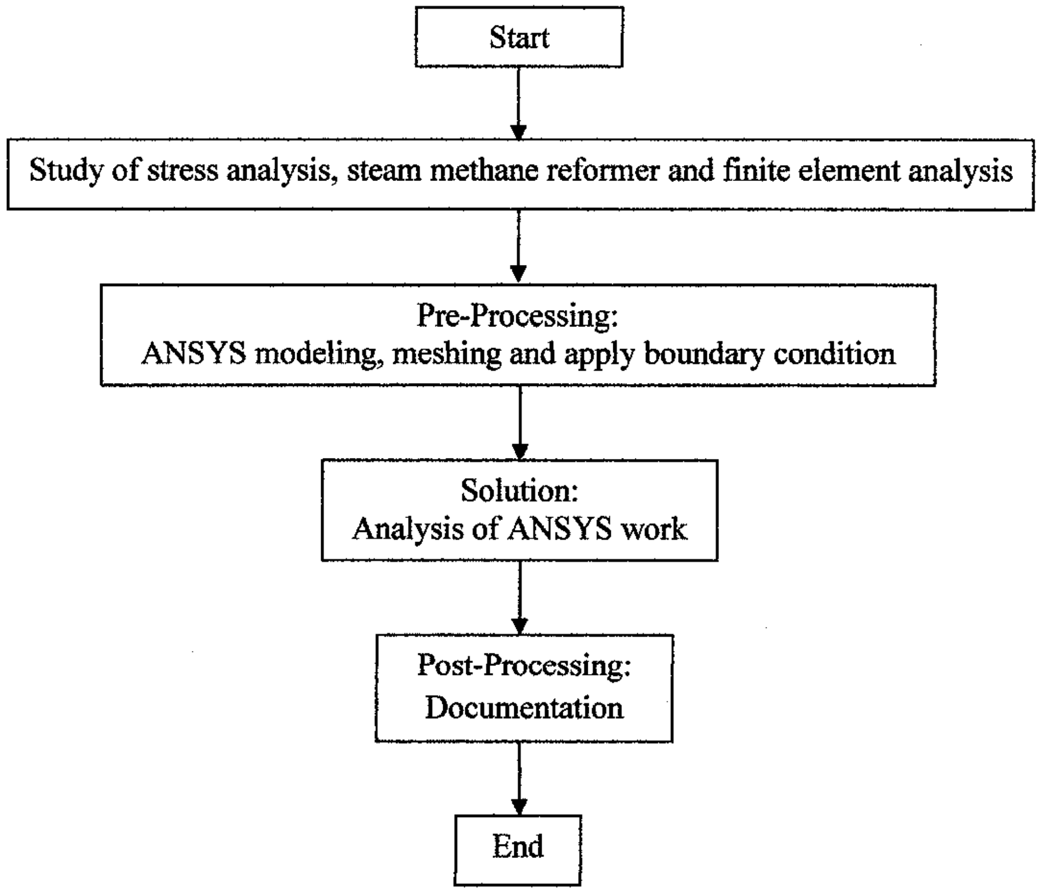

Figure 3.1: Project Flow Chart

The parameters of the tube are like this:

- Inner radius, r_i= 52.5 mm
- Outer radius, r_o= 62.5 mm
- Tube length, l= 12.5 m
- Young Modulus=105 x 10^9

There were two types of analysis have been conducted during completing this project which are stress analysis and thermal stress analysis. The first analysis which is stress analysis has been conducted to determine the Von Misses Stress along the tube due to internal pressure inside the tube while latter on the second analysis which is thermal analysis has been conducted to determine Von Misses Stress along the tube due to temperature profile and internal pressure along the tube. For the stress analysis, since the tube is axially symmetric about its central axis, an axisymmetric analysis will be performed using two-dimensional, 8-node quadrilateral elements (Plane 82) with the axisymmetric option activated. In addition, the tube is symmetric about a plane through the center of the cylinder. Thus, only a quarter section of the tube needs to be modeled. So, for 2D model, the left hand side of the model was the inner radius of the tube while at the right hand site of the model was the outer radius of the tube as shown in Figure 3.2. The size of element used to mesh the model has been fixed to 0.005 mm to ensure the result obtained is accurate enough. The meshed model as shown below:

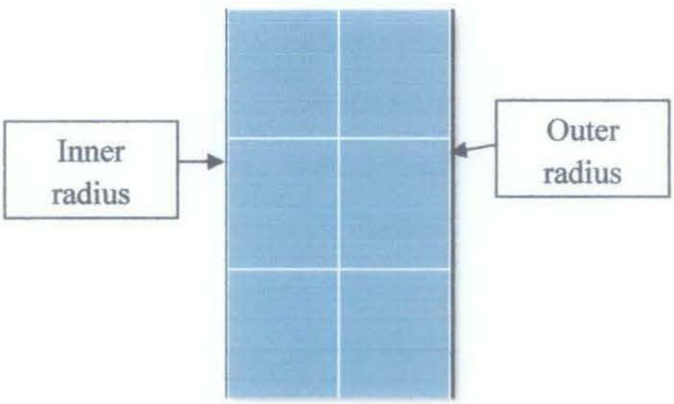

Figure 3.2: Element in 2D model

Figure 3.3: Element in ¾ expansion of 2D axisymmetric model

After the model has been meshed, then the next step taken was applied boundary condition to this model. This model has been compared to the actual tube in real operating condition. In reality, the top of the tube has been hold by other equipment meaning the top of the tube cannot be elongate to the y-axis but can still expand to the x-axis. In contrast, the bottom part of the tube is in free condition which means that it can expand and elongate along the x-axis and y-axis. So, refer to the actual condition, the 2D model has been fixed at the top with the y-axis displacement is equal to zero while at the bottom of the tube, neither both axis have been fixed as shown in Figure 3.4.

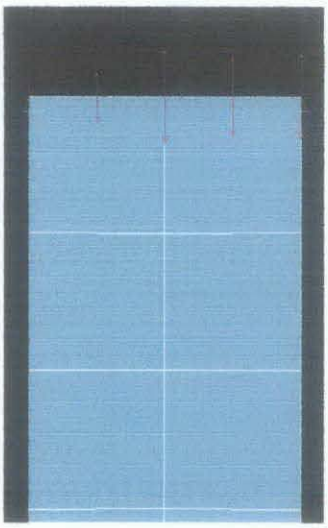

Figure 3.4: y-axis was fixed at zero displacement

The next step was applied internal pressure on the model. Since the left part of the tube is the inner radius, then the internal pressure has been applied to the left line of the model as shown in Figure 3.5.

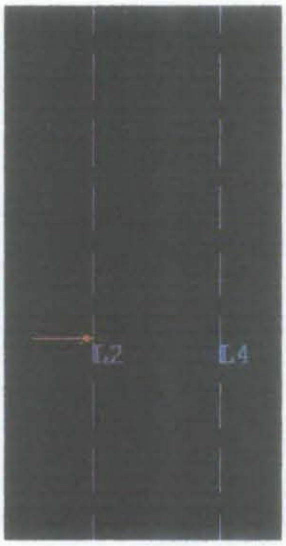

Figure 3.5: Internal pressure at the inner radius of tube

After the pre-processing stage, the next stage is solution stage where the model has been solved. The result of the analysis then will be analyzed in post-processing stage. In post-processing stage, the FEM result has been compared to the analytical result. For the second analysis which is thermal stress, the same step has been taken although some parameters have been changed. The model is still in axisymetric analysis and the type of element used has been changed to 8-node quadrilateral elements (Plane 183) with the axisymmetric option activated. The next step was applied both sides of the model with temperature as shown in Figure 3.6.

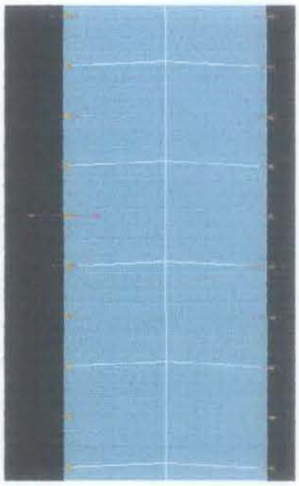

Figure 3.6: Temperature distribution along tube

Similar to the stress analysis, the next step after the boundary conditions has been applied was to solved the model. Then the result was analyzed by comparing the FEM result with the analytical result.

3.3 Gantt Chart

Figure 3.7 show the Gantt chart of the project.

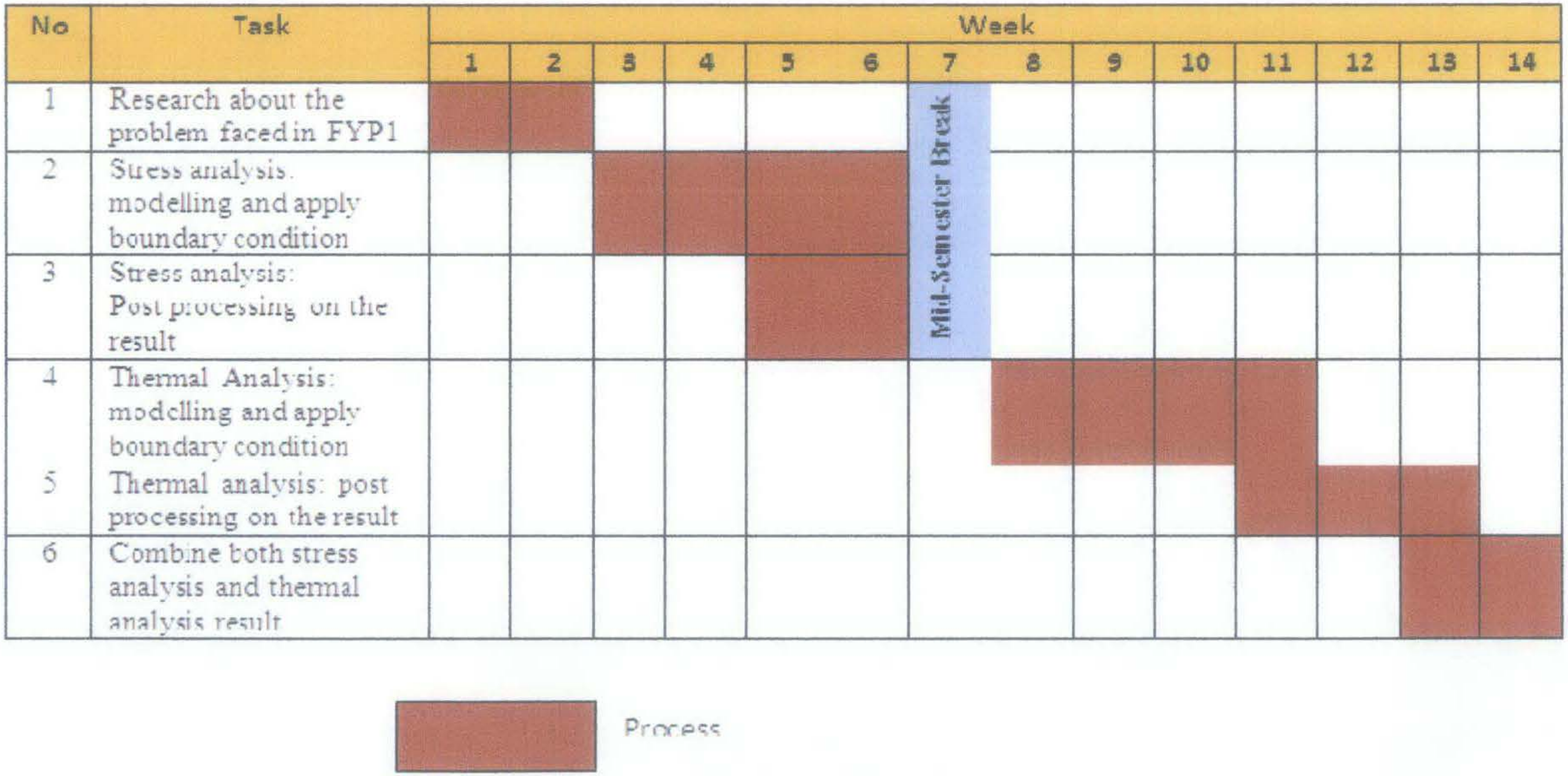

Figure 3.7: Gantt chart

CHAPTER 4

RESULT & DISCUSSION

Below are the input parameters that have been applied to the ANSYS model.

Table 4.1: Modeling parameters for the tube.

Sample	Distance from Top Flange, m	p,MPa	T, K
N1-I N1-O	2.5	2.16	1048 1121
N2-I N2-O	5.0	2.07	1097 1151
N3-I N3-O	7.5	1.99	1119 1151
N4-I N4-O	10.0	1.91	1141 1159
N5-I N5-O	12.5	1.82	1151 1161

(Note: Samples N1 through N5 represent locations at 2.5 intervals starting at 2.5m to 12.5m from the top inlet flange. I and O represent 'inner wall' and 'outer wall' locations respectively).

The material properties of the tube are as shown below:

Density, $\rho = 8.0\text{g/cm}^3$

Thermal Conductivity, k= 14.6 W/mK

Poisson's ratio,v=0.3

Young Modulus=105 x 10^9 Pa

4.1 Analytical Result of Stress Analysis

The Von Misses Stress data for the analytical results is shown in Table 4.2 and Figure 4.1 below:

Table 4.2: Analytical stress due to internal pressure

Sample ID	Pressure (MPa)	r (mm)	σ_h (MPa)	σ_a (MPa)	σ_r (MPa)	σ_o (MPa)
N1-I	2.16	52.5	12.49	5.19	-2.16	12.69
N1-mid		57.5	11.27	5.17	-0.94	10.57
N1-O		62.5	10.33	5.17	0.00	8.95
N2-I	2.07	52.5	12.01	4.97	-2.07	12.19
N2-mid		57.5	10.84	4.97	-0.90	10.17
N2-O		62.5	9.94	4.97	0.00	8.61
N3-I	1.99	52.5	11.53	4.77	-1.99	11.71
N3-mid		57.5	10.40	4.77	-0.87	9.76
N3-O		62.5	9.54	4.77	0.00	8.26
N4-I	1.91	52.5	11.04	4.57	-1.91	11.22
N4-mid		57.5	9.97	4.57	-0.83	9.35
N4-O		62.5	9.14	4.57	0.00	7.92
N5-I	1.82	52.5	10.56	4.37	-1.82	10.72
N5-mid		57.5	9.53	4.37	-0.79	8.94
N5-O		62.5	8.74	4.37	0.00	7.57

(Note: Samples N1 through N5 represent locations at 2.5 intervals starting at 2.5m to 12.5m from the top inlet flange. I and O represent 'inner wall', 'mid wall' and 'outer wall' locations respectively).

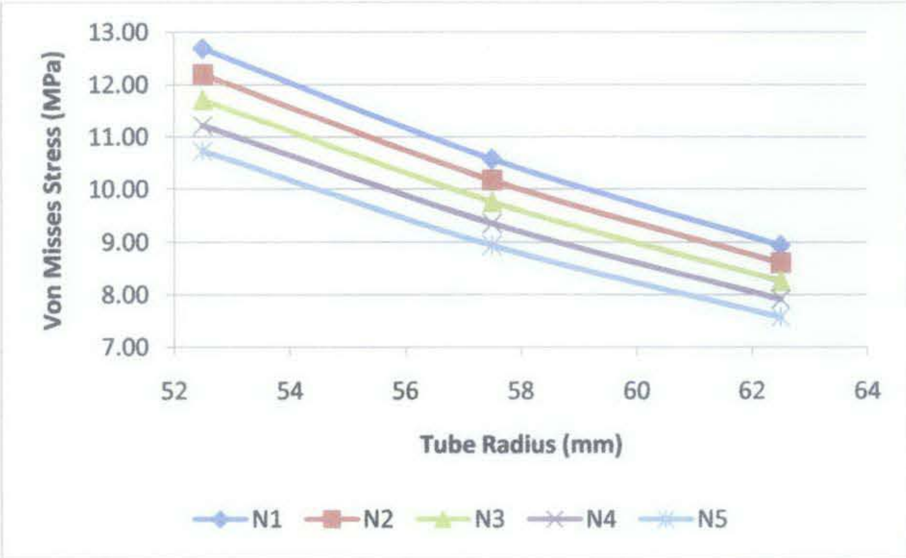

Figure 4.1: Graph of analytical Von Misses Stress

From the graph shown above, the Von Misses Stress is decrease from the inner radius through to the outer radius and also decreases from the top to the bottom of the tube.

For comparison purpose, data from three locations for every interval of 2.5 m on the model have been collected. The reason three locations have been collected is because the analytical result is not affected by length of the tube meaning that it will show a constant value along the interval of 2.5 m of the tube.

$$\text{hoop stress}: \quad \sigma_{hp} = \frac{pr_i^2}{r_o^2 - r_i^2}\left(1 + \frac{r_o^2}{r^2}\right)$$

$$\text{radial stress}: \quad \sigma_{rp} = \frac{pr_i^2}{r_o^2 - r_i^2}\left(1 - \frac{r_o^2}{r^2}\right)$$

$$\text{axial stress}: \quad \sigma_{ap} = \frac{pr_i^2}{r_o^2 - r_i^2}$$

From the equation,the analytical equation is only affected by the change in internal pressure, inner radius and outer radius of the tube. Besides, the analytical assume that both end of the tube have a same boundary condition which will produce a constant stress along the tube. However, because of the different in boundary conditions of both end, the Von Misses Stress are not constant along the tube. The three locations that have been selected to compare the result with the analytical result are the locations where the first node of the internal pressure applied, the locations where the last node of the same internal pressure applied and lastly, the locations where the node is at the intersection between two different internal pressures.

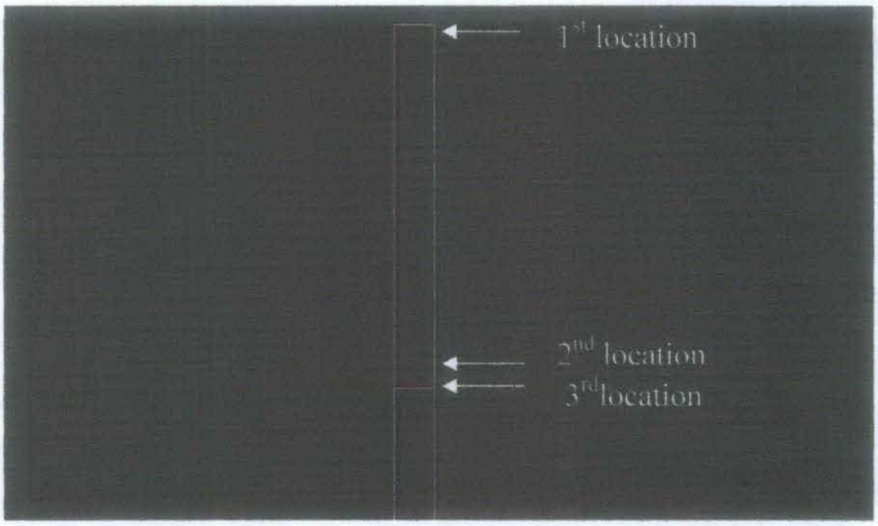

Figure 4.2: Three selected data locations to be collected

4.2 FEM Result of Stress Analysis

Nodal solutions of the stress analyses are shown in Figure 4.3.

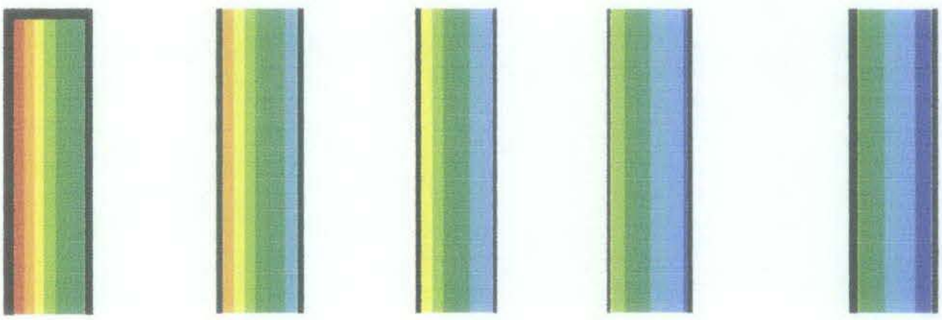

Top- 2.5 m 2.5 m- 5 m 5 m – 7.5 m 7.5 m- 10 m 10 m- 12.5 m

Figure 4.3: Nodal Solution of the stress analysis from top to bottom of the tube

1st location data

From the result shown in Table 4.3, the Von Misses Stress at the 1st location is in similar pattern as the analytical result which shown that the Von Misses Stress is decreasing from the inner radius through to the outer radius and also decreasing from the top to the bottom of the tube. However, the magnitude of the Von Misses Stress for the FEM data is higher than the analytical data with the error percentage is below 10% for all locations along the tube.

Table 4.3: 1st location result

Sample ID	Pressure,p,MPa	r (mm)	FEM σ_o ,(Pa)	Analytical σ_o ,(Pa)	Error (%)
N1-I	2.16	52.5	1.37E+07	1.25E+07	8.89
N1-mid		57.5	1.18E+07	1.13E+07	4.13
N1-O		62.5	1.03E+07	1.03E+07	-0.04
N2-I	2.07	52.5	1.33E+07	1.20E+07	9.60
N2-mid		57.5	1.14E+07	1.08E+07	5.14
N2-O		62.5	1.01E+07	9.94E+06	1.28
N3-I	1.99	52.5	1.28E+07	1.15E+07	9.63
N3-mid		57.5	1.10E+07	1.04E+07	5.22
N3-O		62.5	9.67E+06	9.54E+06	1.31
N4-I	1.91	52.5	1.23E+07	1.10E+07	9.90
N4-mid		57.5	1.05E+07	9.97E+06	5.39
N4-O		62.5	9.28E+06	9.14E+06	1.56
N5-I	1.82	52.5	1.15E+07	1.06E+07	8.36
N5-mid		57.5	9.90E+06	9.53E+06	3.78
N5-O		62.5	8.70E+06	8.74E+06	-0.46

2nd location data

From the result shown in Table 4.4, the Von Misses Stress at the 2nd location is in similar pattern as the analytical result which shown that the Von Misses Stress is decreasing from the inner radius through to the outer radius and also decreasing from the top to the bottom of the tube. However, the magnitude of the Von Misses Stress for the FEM data is higher than the analytical data and the error percentage is below 10% for all locations along the tube.

Table 4.4: 2nd location result

Sample ID	Pressure,p,MPa	r (mm)	FEM σ_o ,(Pa)	Analytical σ_o ,(Pa)	Error (%)
N1-I		52.5	1.36E+07	1.25E+07	8.11
N1-mid	2.16	57.5	1.16E+07	1.13E+07	3.13
N1-O		62.5	1.02E+07	1.03E+07	-1.29
N2-I		52.5	1.29E+07	1.20E+07	7.22
N2-mid	2.07	57.5	1.11E+07	1.08E+07	2.39
N2-O		62.5	9.74E+06	9.94E+06	-2.03
N3-I		52.5	1.24E+07	1.15E+07	7.30
N3-mid	1.99	57.5	1.07E+07	1.04E+07	2.53
N3-O		62.5	9.36E+06	9.54E+06	-1.92
N4-I		52.5	1.19E+07	1.10E+07	7.32
N4-mid	1.91	57.5	1.02E+07	9.97E+06	2.49
N4-O		62.5	8.96E+06	9.14E+06	-2.03
N5-I		52.5	1.17E+07	1.06E+07	9.77
N5-mid	1.82	57.5	1.01E+07	9.53E+06	5.42
N5-O		62.5	8.87E+06	8.74E+06	1.50

3rd location data

From the result shown in Table 4.5, the Von Misses Stress at the 3rd location is in similar pattern as the analytical result which shown that the Von Misses Stress is decreasing from the inner radius through to the outer radius and also decreasing from the top to the bottom of the tube. However, the magnitude of the Von Misses Stress for the FEM data is higher than the analytical data and the error percentage is below 10% for all locations along the tube.

In comparing the results of all these three locations in Figure 4.4, the result showed that all three locations have approximately the same magnitude of Von Misses Stress. The reason of the difference in values of the FEM result with the analytical result is because the analytical equation does not include other variables that should be considered while conducting this analysis such as the boundary conditions.

Table 4.5: 3rd location result

Sample ID	Pressure,p,MPa	r (mm)	FEM, σ_o (MPa)	Analytical σ_o (MPa)	Error (%)
N1-I	2.16	52.5	1.34E+07	1.25E+07	6.95
N1-mid		57.5	1.15E+07	1.13E+07	2.02
N1-O		62.5	1.01E+07	1.03E+07	-2.17
N2-I	2.07	52.5	1.29E+07	1.20E+07	6.55
N2-mid		57.5	1.10E+07	1.08E+07	1.81
N2-O		62.5	9.70E+06	9.94E+06	-2.43
N3-I	1.99	52.5	1.23E+07	1.15E+07	6.61
N3-mid		57.5	1.06E+07	1.04E+07	1.93
N3-O		62.5	9.32E+06	9.54E+06	-2.34
N4-I	1.91	52.5	1.18E+07	1.10E+07	6.50
N4-mid		57.5	1.02E+07	9.97E+06	1.78
N4-O		62.5	8.92E+06	9.14E+06	-2.52
N5-I	1.82	52.5	1.15E+07	1.06E+07	8.36
N5-mid		57.5	9.90E+06	9.53E+06	3.78
N5-O		62.5	8.70E+06	8.74E+06	-0.46

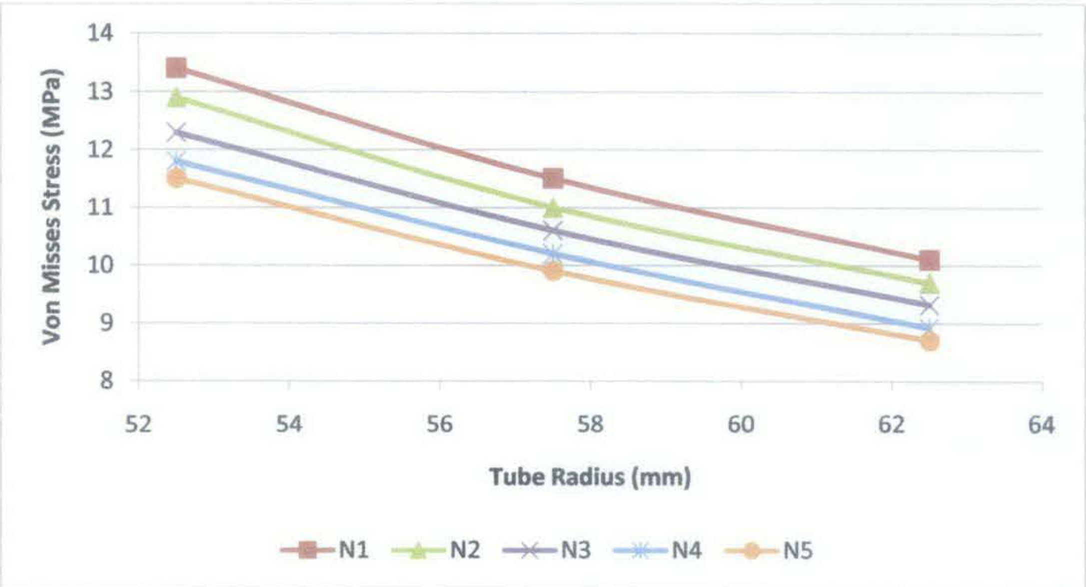

Figure 4.4: Graph of 3rd location results

4.3 Analytical Result of Thermal Analysis

The results of analytical calculations of stresses due to temperature profile of the tube are shown in Table 4.6.

Table 4.6: Thermal Analysis results

Sample ID	Pressure (MPa)	r (mm)	σ_h (MPa)	σ_a (MPa)	σ_r (MPa)
N1-I	2.16	52.5	99.05	99.05	0
N1-mid		57.5	-2.7	1.35	4.05
N1-O		62.5	-88.19	-88.19	0
N2-I	2.07	52.5	72.27	72.27	0
N2-mid		57.5	-1.97	0.99	2.96
N2-O		62.5	-64.35	-64.35	0
N3-I	1.99	52.5	42.18	42.18	0
N3-mid		57.5	-1.15	0.58	1.73
N3-O		62.5	-37.56	-37.56	0
N4-I	1.91	52.5	24.75	24.75	0
N4-mid		57.5	-0.67	0.34	1.01
N4-O		62.5	-22.04	-22.04	0
N5-I	1.82	52.5	12.84	12.84	0
N5-mid		57.5	-0.35	0.18	0.53
N5-O		62.5	-11.43	-11.43	0

4.4 Analytical Result of Thermal Stress Analysis

The results of analytical calculations of stresses due to temperature profile and internal pressure of the tube are shown in Table 4.7, and graphically in Figure 4.5.From the graph shown, the Von Misses Stress at the same interval is highest at the inner radius and lowest at the mid wall. Besides, the result showed that the Von Misses Stress is higher at the inner radius compare to Von Misses Stress at the outer radius. The Von Misses Stress is decreasing from the inner radius to the mid radius but then rise back to the outer radius. In addition, the Von Misses Stress is highest at the top of the tube and lowest at bottom. The other observation is for sample N5 which is the sample at interval 12.5 m from the top flange of the tube, the Von Misses Stress is keep decreasing from the inner radius through to the outer radius.

Table 4.7: Thermal Stress Analysis results

Sample ID	Pressure (Mpa)	r (mm)	σ_h (Mpa)	σ_a (Mpa)	σ_r (MPa)	σ_o ,(Pa)
N1-I	2.16	52.5	111.54	104.17	-2.16	1.10E+08
N1-mid		57.5	8.57	6.47	3.11	4.77E+06
N1-O		62.5	-77.86	-83.07	0	8.06E+07
N2-I	2.07	52.5	84.28	77.14	-2.07	8.30E+07
N2-mid		57.5	8.87	5.86	2.06	5.91E+06
N2-O		62.5	-54.41	-59.48	0	5.71E+07
N3-I	1.99	52.5	53.71	46.8	-1.99	5.26E+07
N3-mid		57.5	9.25	5.2	0.86	7.29E+06
N3-O		62.5	-28.02	-32.94	0	3.08E+07
N4-I	1.91	52.5	35.8	29.12	-1.91	3.49E+07
N4-mid		57.5	9.29	4.71	0.18	7.89E+06
N4-O		62.5	-12.9	-17.66	0	1.58E+07
N5-I	1.82	52.5	23.4	16.96	-1.82	2.27E+07
N5-mid		57.5	9.18	4.3	-0.27	8.19E+06
N5-O		62.5	-2.69	-7.31	0	6.40E+06

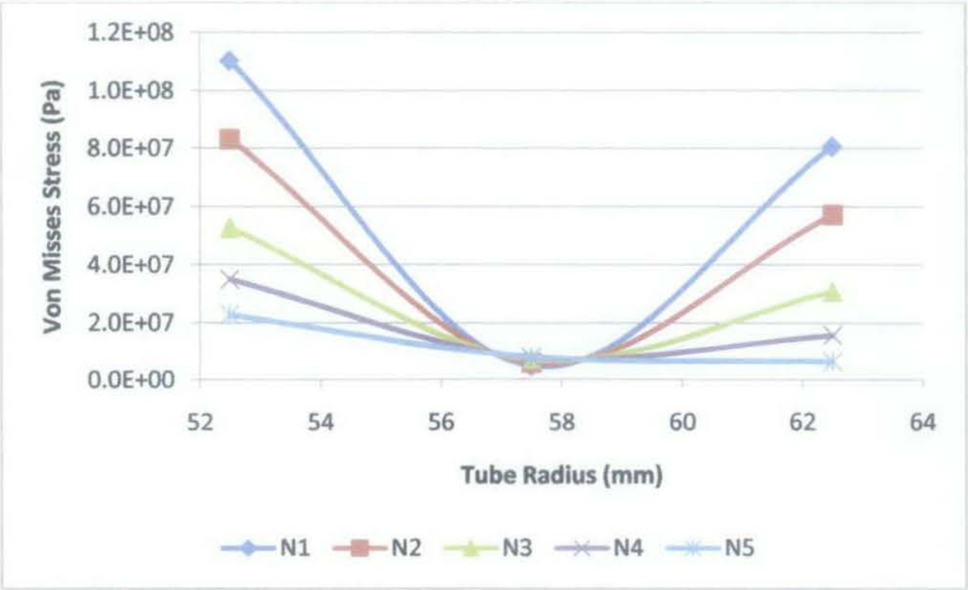

Figure 4.5: Graph of thermal analysis results

4.5 FEM Result of Thermal Stress Analysis

Nodal solutions of the stress and thermal analyses are shown in Figure 4.6.

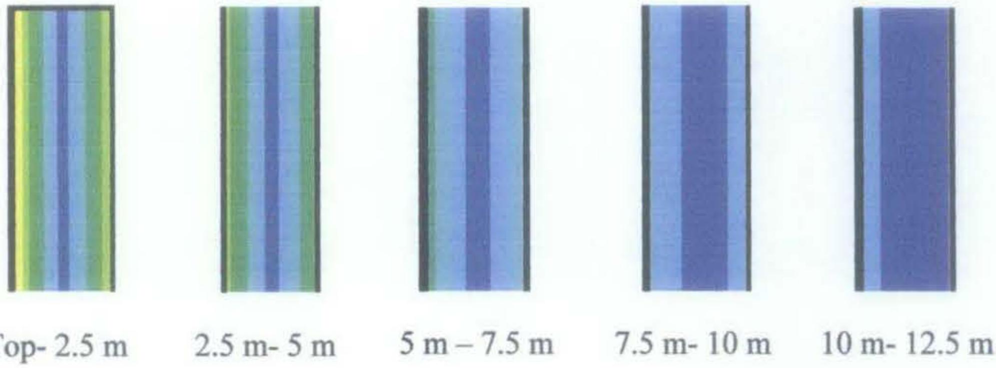

Figure 4.6: Nodal Solution of the thermal stress analysis from top to bottom of the tube

<u>1st location data</u>

From the data shown in Table 4.8 and Figure 4.7 below, the Von Misses Stress at the same interval is decreasing from the inner radius to the mid radius but then rise back to the outer radius. Besides, at the same interval, the lowest Von Misses Stress is at the mid wall radius of the tube. Other than that, it is also observed that the Von Misses Stress is highest at the top of the tube and lowest at bottom. Lastly, it is obvious that the Von Misses Stress at the mid wall radius at interval of 2.5 from the top of tube is lowest than the Von Misses Stress at mid wall radius of interval 5 m, 7.5m and 10 m but higher than Von Misses Stress at mid wall radius of interval 12.5 m from the top flange. This is because of the boundary condition set at the top of the tube as the boundary condition effect the Von Misses Stress.

Table 4.8: 1st location results

Sample ID	Pressure, p, MPa	r (mm)	FEM, σ_o (Pa)	Analytical, σ_o (Pa)	Error (%)
N1-I	2.16	52.5	1.36E+08	1.14E+08	16.27
N1-mid		57.5	4.59E+06	5.46E+06	-18.94
N1-O		62.5	1.13E+08	8.31E+07	26.79
N2-I	2.07	52.5	7.73E+07	8.64E+07	-11.64
N2-mid		57.5	2.57E+07	6.81E+06	73.52
N2-O		62.5	1.01E+08	5.95E+07	41.38
N3-I	1.99	52.5	6.23E+07	5.57E+07	10.59
N3-mid		57.5	7.94E+06	8.39E+06	-5.68
N3-O		62.5	5.91E+07	3.29E+07	44.30
N4-I	1.91	52.5	3.13E+07	3.77E+07	-20.32
N4-mid		57.5	7.48E+06	9.11E+06	-21.85
N4-O		62.5	3.41E+07	1.77E+07	48.14
N5-I	1.82	52.5	1.85E+07	2.52E+07	-36.43
N5-mid		57.5	4.68E+06	9.45E+06	-102.04
N5-O		62.5	7.26E+06	7.31E+06	-0.70

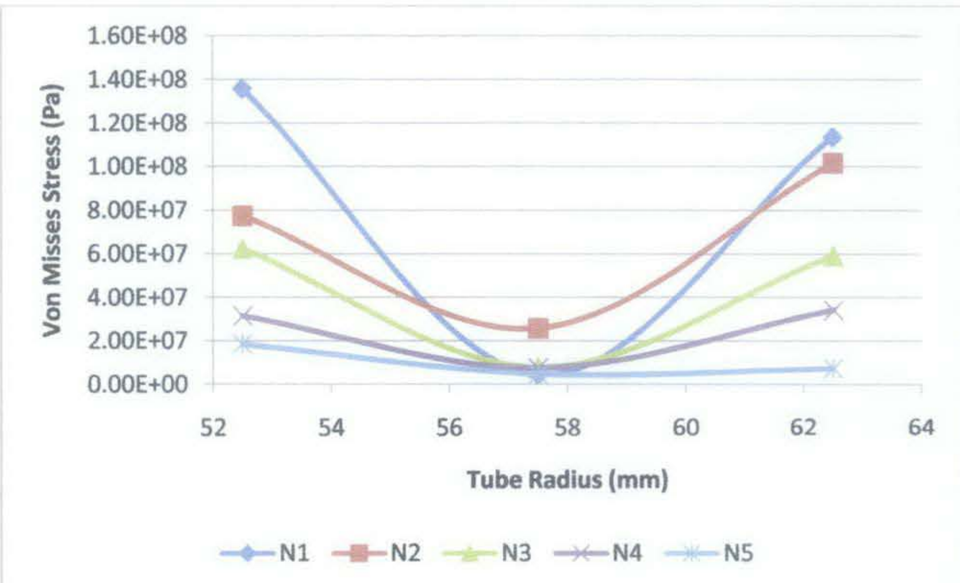

Figure 4.7: Graph of 1st location results

2nd location data

From the data shown in Table 9 and Figure 4.8 below, the Von Misses Stress at the same interval is highest at the inner radius and lowest at the mid wall. Besides, the result showed that the Von Misses Stress is higher at the inner radius compare to

Von Misses Stress at the outer radius. The Von Misses Stress is decreasing from the inner radius to the mid radius but then rise back to the outer radius. In addition, the Von Misses Stress is highest at the top of the tube and lowest at bottom.

Table 4.9: 2nd location results

Sample ID	Pressure, p, MPa	r (mm)	FEM, σ_o (Pa)	Analytical σ_o (Pa)	Error (%)
N1-I	2.16	52.5	1.57E+08	1.14E+08	27.67
N1-mid		57.5	2.78E+07	5.46E+06	80.38
N1-O		62.5	1.20E+08	8.31E+07	30.59
N2-I	2.07	52.5	1.12E+08	8.64E+07	22.74
N2-mid		57.5	1.36E+07	6.81E+06	49.90
N2-O		62.5	7.28E+07	5.95E+07	18.32
N3-I	1.99	52.5	8.02E+07	5.57E+07	30.57
N3-mid		57.5	1.63E+07	8.39E+06	48.51
N3-O		62.5	4.17E+07	3.29E+07	21.08
N4-I	1.91	52.5	4.68E+07	3.77E+07	19.48
N4-mid		57.5	1.19E+07	9.11E+06	23.26
N4-O		62.5	2.29E+07	1.77E+07	22.80
N5-I	1.82	52.5	2.25E+07	2.52E+07	-11.96
N5-mid		57.5	5.31E+06	9.45E+06	-78.11
N5-O		62.5	1.74E+07	7.31E+06	57.93

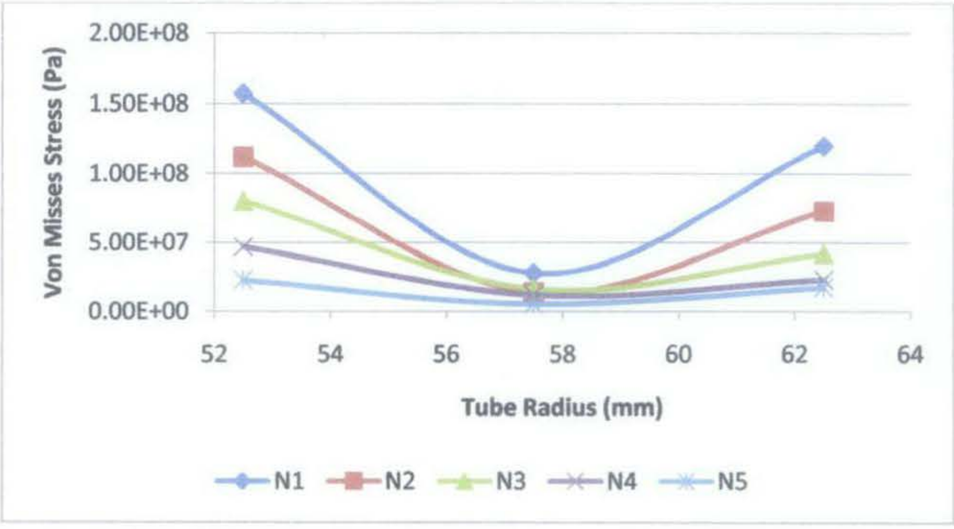

Figure 4.8: Graph of 2nd location results

3^{rd} location data

From the shown in Table 4.10 and Figure 4.9 below, the Von Misses Stress at the same interval is highest at the inner radius and lowest at the mid wall. Besides, the result showed that the Von Misses Stress is higher at the inner radius compare to Von Misses Stress at the outer radius. The Von Misses Stress is decreasing from the inner radius to the mid radius but then rise back to the outer radius. In addition, the Von Misses Stress is highest at the top of the tube and lowest at bottom. Besides, the result shown that the FEM result obtained has large error in N5 sample's data which showed that there must be some modification have to be made in the model especially in the boundary condition.

Table 4.10: 3^{rd} location results

Sample ID	Pressure,p,MPa	r (mm)	FEM σ_o (Pa)	Analytical σ_o (Pa)	Error (%)
N1-I	2.16	52.5	1.10E+08	1.14E+08	-3.70
N1-mid		57.5	2.29E+07	5.46E+06	76.19
N1-O		62.5	1.01E+08	8.31E+07	17.82
N2-I	2.07	52.5	7.85E+07	8.64E+07	-9.95
N2-mid		57.5	1.25E+07	6.81E+06	45.60
N2-O		62.5	6.48E+07	5.95E+07	8.22
N3-I	1.99	52.5	4.69E+07	5.57E+07	-18.74
N3-mid		57.5	1.31E+07	8.39E+06	35.83
N3-O		62.5	3.67E+07	3.29E+07	10.18
N4-I	1.91	52.5	3.00E+07	3.77E+07	-25.69
N4-mid		57.5	9.59E+06	9.11E+06	5.03
N4-O		62.5	1.94E+07	1.77E+07	8.98
N5-I	1.82	52.5	1.36E+07	2.52E+07	-85.40
N5-mid		57.5	3.91E+05	9.45E+06	-2316.01
N5-O		62.5	1.14E+07	7.31E+06	36.08

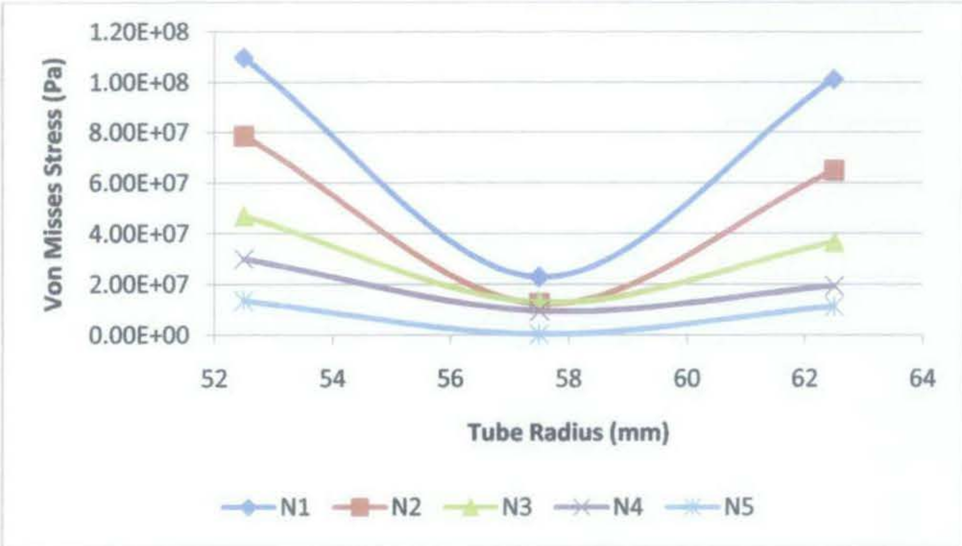

Figure 4.9: Graph of 3rd location results

CHAPTER 5
CONCLUSION& RECOMMENDATION

As for conclusion, the result generally showed the same pattern or profile with the analytical result. The only concern is for the magnitude of the result especially for thermal stress analysis. There are still some modifications have to be made on the model since the thermal analysis result do not obtained the desired result. The modifications might focus on the boundary conditions of the model since there are many other possibilities for the boundary conditions in this model that have to be considered. Besides, the size of the element can also help to increase the accuracy of the result.

For thermal stress analysis, other variables should be considered too such as the convection and radiation properties of the material. This is because the heat transfer in the tube may occur through convection, conduction and radiation. These variables are very essential to determine the Von Misses Stress along the tube so that can be used to determine the service life of the reformer tube.

REFERENCES

1. AIA: Software Analyzes Cost of Hydrogen Production, 1 January 2004, < www.assemblymag.com>.
2. Ashok Kumar Ray Samarendra Kumar Sinha, Yogendra Nath Tiwari, Jagannathan Swaminathan, Gautam Das, Satyabrata Chaudhuri and Raghubir Singh, 2003, Analysis of failed reformer tubes.
3. Azmi Abdul Wahab, 2007, Three-dimensional analysis of creep void formation in steam-methane reformer tubes.
4. Baher El Shaikh, 2010, Steam Reformer Design, Fabrication and Erection.
5. David N. French,July 1991,"Creep and Creep Failures" in National Board Bulletin
6. Deborah A. Kramer, 2005, Mineral Commodity Summaries.
7. George W. Crabtree, Mildred S. Dresselhaus, and Michelle V. Buchanan, "The Hydrogen Economy", Physics Today, December, 2004
8. Hydrogen Production- Steam Methane Reforming, 2010, www.getenergysmart.org
9. Morozov, E.M. and Fridman, I.B., Thermal stresses and their calculation, in Strength and deformation in nonuniform temperature fields; a collection of scientific papers, Fridman, I.B., Editor. 1964, Consultants Bureau: New York.
10. Muvdi, B.B. and McNabb, J.W., Engineering mechanics of materials. 3rd ed.1991, New York: Springer-Verlag.
11. Schmidt + Clemens, Centralloy CA4852-Micro material data sheet. 2001, Schmidt + Clements Group: Lindlar-Kaiserau, Germany.
12. Steve Roensch, 2008, The Finite Element Method.<www.finiteelement.com>
13. Strength of material-Mechanic of Material, 15 August 2010, <http://www.engineersedge.com/strength_of_materials.htm>